A&A 439, 29–33 (2005)
DOI: 10.1051/0004-6361:20042112

Astronomy & Astrophysics

Galaxy populations of double cluster RX J1053.7+5735 at $z = 1.13$

Yasuhiro Hashimoto[1], J. Patrick Henry[1,2], G. Hasinger[1], G. Szokoly[1], and M. Schmidt[3]

[1] Max-Planck-Institut für extraterrestrische Physik, Giessenbachstrasse 85748 Garching, Germany
e-mail: hashimot@mpe.mpg.de
[2] Institute for Astronomy, University of Hawaii, 2680 Woodlawn Drive, Honolulu, Hawaii 96822, USA
[3] Palomar Observatory, California Institute of Technology, MS 320-47 Pasadena, CA 91125, USA

Received 4 October 2004 / Accepted 23 February 2005

Abstract. We present a study of the galaxy population in the cluster RX J1053.7+5735, one of the most distant X-ray selected clusters of galaxies and one which also shows an unusual double-lobed X-ray morphology, indicative of a possible equal-mass cluster merger. The cluster was discovered during the *ROSAT* deep pointings in the direction of the Lockman Hole. Using Keck-DEIMOS spectroscopic observations of galaxies in the $2\farcm0 \times 1\farcm5$ region surrounding RX J1053.7+5735, we secured redshifts for six galaxies in the range $1.129 < z < 1.139$, with a mean redshift $\langle z \rangle = 1.134$. This mean redshift agrees well with the cluster *X-ray* redshift previously estimated from the cluster X-ray Fe-K line, confirming the presence of a cluster at $z \sim 1.135$. Galaxies with concordant redshifts are located in both eastern and western sub-clusters of the double cluster structure, which indicates that both sub-clusters are at similar redshifts. This result is also consistent with a previous claim that both eastern and western X-ray lobes have similar X-ray redshifts. Based on their separation of ∼250 kpc, these results support the interpretation that RX J1053.7+5735 is an equal-mass cluster merger taken place at $z \sim 1$, although further direct evidence for a dynamical state of the cluster is needed to make a more definitive statement about the cluster merging state. The six galaxies have a line-of-sight velocity dispersion $\Delta v \sim 650$ km s^{-1}, and all six show clear absorption features of CaII H and K and several Balmer lines that are typical of early galaxies at the present epoch, in agreement with their $I - K$ colors. A color–magnitude diagram, constructed from deep optical/NIR observations of the RX J1053.7+5735 field, shows a clear red color sequence. There is an indication that the red sequence in RX J1053.7+5735 lies ∼0.3 to the blue of the Coma line, qualitatively consistent with previous studies investigating other clusters at $z \sim 1$.

Key words. galaxies: clusters: general – galaxies: high-redshift – infrared: galaxies – X-rays: galaxies: clusters – galaxies: evolution – galaxies: stellar content

1. Introduction

Identification and study of distant galaxy clusters is of great interest in current astronomical research. As the most massive collapsed objects in the universe, clusters provide a sensitive probe of the formation and evolution structure in the universe (Eke et al. 1996; Bahcall et al. 1997). The presence of clusters or large-scale structures at and beyond $z = 1$ can constrain scenarios for bottom-up structure formation and fundamental cosmological parameters by requiring cluster-level collapse earlier than that epoch. Another equally important use of galaxy clusters lies in studying the formation and evolution of galaxy populations. The study of the spectral and photometric properties of cluster galaxies at large redshifts provides a powerful means of discriminating between scenarios for the formation of elliptical galaxies. Predictions of the color–magnitude distribution of cluster early-types galaxies based on hierarchical models of galaxy formation (Kauffmann 1996; Kauffmann & Charlot 1998) differ at $z > 1$ from models in which ellipticals formed at high-z in a monolithic collapse (Eggen et al. 1962). Meanwhile, studying individual galaxies in high-z clusters can also provide information on the cluster environment, and on merging and star formation history in the cluster galaxies, and provide samples of cluster ellipticals and spirals which could be compared with field galaxies at the high redshift and cluster galaxies at low redshift.

The cluster RX J1053.7+5735, which shows an unusual double-lobed X-ray morphology, was discovered during deep (1.31 Ms) *ROSAT* HRI pointings (Hasinger et al. 1998a) in the direction of the "Lockman Hole", a line of sight with exceptionally low HI column density (Lockman et al. 1986). The angular size of the source is 1.7×0.7 arcmin^2, and two lobes are approximately 1 arcmin apart. The total X-ray flux of the entire source in the 0.5–2.0 keV band is 2×10^{-14} erg cm^{-2} s^{-1} (Hasinger et al. 1998b). Subsequent deep optical/NIR imaging follow-ups ($V < 26.5$, $R < 25$, $I < 25$, $K < 20.5$) with LRIS/NIRC on Keck and Calar Alto Omega Prime camera revealed a bright 7 arcsecond-long arc with a magnitude of $R = 21.4$, as well as an overdensity of galaxies in both X-ray lobes (e.g. Thompson et al. 2001). Further Keck LRIS/NIRSPEC spectroscopic observations of the bright arc and one of the brightest galaxies near the arc showed that the former is a lensed galaxy at a redshift $z = 2.57$, while the latter may be at

a redshift of $z = 1.263$ (Thompson et al. 2001). Deep *VRIzJHK* photometry data produced concordant photometric redshifts for more than 10 objects at redshift of $z \sim 1.1-1.3$, confirming that at least the eastern lobe is a massive cluster at high redshift. The improbability of chance alignment and similarity of colors for the galaxies in the two X-ray lobes were consistent with the western lobe also being at $z \sim 1.1-1.3$ (Thompson et al. 2001).

The X-ray data of the XMM-Newton (XMM) observation (with a total effective exposure time ∼100 ks) performed during the PV phase for this cluster were analyzed (Hashimoto et al. 2002) and yield a best-fit temperature of $4.9^{+1.5}_{-0.9}$ keV, while the metallicity was poorly constrained with an upper limit on the iron abundance of 0.62 $Z_\odot$. Hashimoto et al. (2004), using even deeper (∼700 ks) XMM observations, detected the Fe K line in the cluster X-ray emission and obtained a strong constraint on cluster metallicity, which is difficult to achieve for clusters at $z > 1$. The best-fit abundance is $0.46^{+0.11}_{-0.07}$ times the solar value. Comparison with other metallicity measurements of nearby and distant clusters showed that there was little evolution in the ICM metallicity from $z \sim 1$ to the present. The Fe line emission also allowed them to directly estimate the redshift of diffuse gas with a value $z = 1.14^{+0.01}_{-0.01}$. This is one of the first clusters whose X-ray redshift is directly measured prior to the secure knowledge of cluster redshift by optical/NIR spectroscopy. Hashimoto et al. (2004) could also estimate the X-ray redshift separately for each of the two lobes in the double-lobed structure, and the result was consistent with the two lobes being part of one cluster system at the same redshift.

Here we report on the optical imaging and spectroscopic follow-up studies of the cluster RX J1053.7+5735 based mainly on our deep observations with 8 m-class telescopes. The paper is organized as follows. In Sect. 2, we briefly describe the observation and data reduction. In Sect. 3, we present imaging and spectroscopic analysis of the cluster RX J1053.7+5735. Sect. 4 summarizes our results. Throughout the paper, we use $H_0 = 65$ km s^{-1} Mpc^{-1}, $\Omega_m = 0.3$, and $\Omega_\Lambda = 0.7$.

2. Observations and data

2.1. Optical and IR imaging

Deep R, I, and Z band images of the region surrounding the cluster RXJ 1053.7+5735 were obtained as a part of IfA Deep Survey (Barris et al. 2004) using the Suprime-Cam (Miyazaki et al. 1998) on the Subaru telescope over ten nights from November 2001 through April 2002. The camera covers a $34' \times 27'$ field of view with a pixel scale of $0''.20$. The Z filter at Subaru has an effective wavelength of 9195 Å and *FWHM* of 1410 Å (Fukugita et al. 1996), while R and I filters are Cousins R and I. The data were taken under various seeing conditions, and we used only images with less than $\sim 0''.8$ seeing. Total effective exposure time after this filtering is 1680s, 2150s, 2640s in R, I, and Z band, respectively. The photometry is calibrated to Vega system using Landolt standards (Landolt 1992). For further details of the Subaru data, please see Barris et al. (2004).

The infrared K (K') images were obtained in Nov. 1994 and Jan. 2002 at the Calar Alto 3.5 m telescope with the Omega-Prime infrared camera, providing a $6'.8$ field of view with $0''.39$ pixels. The flux scale was calibrated using five UKIRT faint standards (Casali & Hawarden 1992) obtained during the January 2002 run. The data were taken using dithered motion with an amplitude of $10''$. The total integration time and seeing of the resulting image are 155 min and $1''.4$.

2.2. Optical spectroscopy

Spectroscopic observations of cluster galaxies were obtained as a part of an optical follow-up program of ∼140 X-ray sources detected in the Lockman Hole, using the Deep Imaging Multi-Object Spectrograph (DEIMOS; Faber et al. 2003) on the Keck II telescope. Four masks were used covering a total of 16×20 arcmin^2 area over a four-night observing-run in February 2004, resulting in a total integration time of ∼8 h for each object. Using one mask covering the cluster region, we assigned four tilted slits to cover eight potential cluster members. No fringing is present in the red for DEIMOS, allowing us to use tilted slits, because there is no need to construct a fringe frame using dithered exposures. Cluster galaxies were assigned slits based mainly on their $I - K$ color and K magnitude. We used the 600 lines mm^{-1} grating blazed at 7150 Å, covering 4550–9700 Å. The dispersion is 0.65 Å/pixel. Spectral resolution depends on the angle of the tilted slit, but is typically ∼6 Å. The slit mask data were separated into individual slitlet spectra and then treated as standard long slit spectral data. The integration is split into a series of 1800 s exposures. The exposures for each slitlet were reduced separately, then coadded. Wavelength calibration of the spectra was obtained from NeXeCdZnHg arc lamp exposures taken during the same night. A flux calibration was obtained from long-slit observations of the standard stars HZ44 and LTT6028.

3. Results

3.1. Photometric properties

Figure 1 shows a color image of a $2'.0 \times 1'.5$ area around the cluster RX J1053.7+5735. The image is composed using R, I, and Z band images taken with Subaru Suprime-Cam. Spectroscopically confirmed members (boxes) and their ids, as well as a position of the gravitational arc, are indicated. The contours are from the X-ray image obtained by XMM, combining all events in the 0.2–8 keV band from three (pn, MOS1, and MOS2) cameras. The lowest contour is 1.9 counts arcsec^{-2}, and the contour interval is 0.2 counts arcsec^{-2}. A catalog of objects in each optical/IR band was obtained using SExtractor (Bertin & Arnouts 1996). The photometry was obtained using a fixed $2''$ aperture. Objects were detected with the requirement that an object area of 2 arcsec^2 must be 1.5σ above the background. Photometric properties of spectroscopically confirmed galaxies, as well as their spectroscopic redshifts, are shown in the Table 1.

Figure 2 shows a color–magnitude diagram for all objects in a $2'.0 \times 1'.5$ field surrounding the cluster RX J1053.7+5735. Colors are based on an I image taken with Subaru Suprime-Cam, and a K image taken with Calar Alto Omega-Prime

Table 1. Properties of Galaxies in RX J1053.7+5735.

ID	RA (10:53:)	Dec (+57:35:)	R (mag)	K (mag)	$R-Z$	$I-K$	Redshift
1	46.88	10.39	23.08	17.21	−0.19	4.44	1.130
2	46.63	14.56	23.68	17.66	−0.08	4.44	1.129
3	44.47	23.79	23.55	18.38	−0.15	3.64	1.139
4	42.26	34.67	23.88	18.29	−0.16	4.06	1.139
5	41.00	12.69	23.86	18.42	−0.32	4.03	1.130
6	40.14	17.77	23.48	17.30	0.00	4.6	1.135

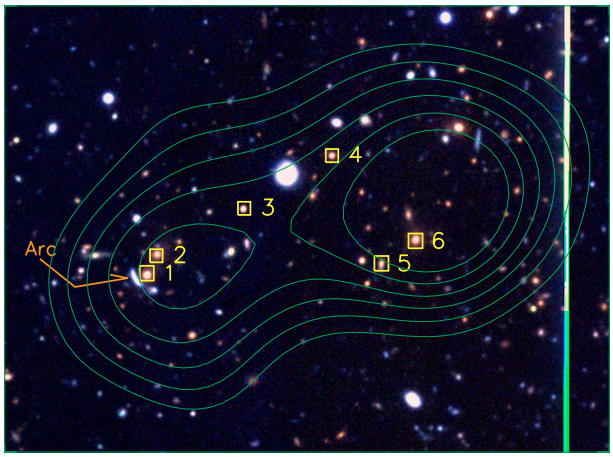

Fig. 1. The color image of 2.′0 × 1.′5 area around the cluster RX J1053.7+5735. The image is composed using R, I, and Z images taken with Subaru Suprime- Cam. North is up and East is left. Spectroscopically confirmed members (boxes) and their ids are shown. The contour is based on the X-ray image obtained by XMM, combining all events in the 0.2–8 keV band from three (pn, MOS1, and MOS2) cameras. The lowest contour is 1.9 counts arcsec^{-2} and the contour interval is 0.2 counts arcsec^{-2}.

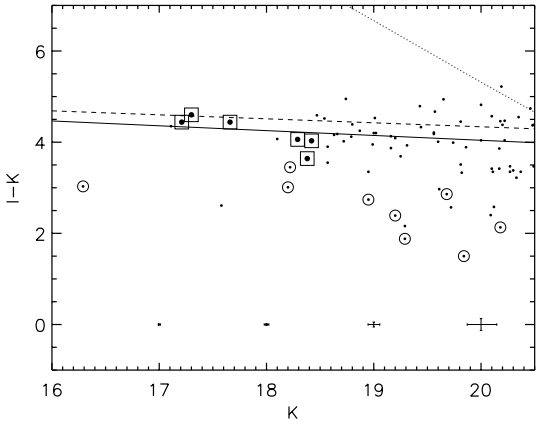

Fig. 2. Color–magnitude diagram for galaxies inside a 2.′0 × 1.′5 field surrounding the cluster RX J1053.7+5735. Colors are based on an I band Subaru Suprime-Cam image and a K band Calar Alto Omega-Prime image. Spectroscopically confirmed members are marked by squares, while spectroscopically known foreground galaxies are marked by circles. The error bars near the bottom of the plot indicate the size of 1σ error. The dotted line marks the 5σ limit in $I-K$ color. The dashed line shows the CM relation of Coma transformed to the cluster redshift assuming no evolution. The solid line is a linear fit to the CM relation of galaxies with $K<20$, $I-K>3$, and $I-K<6$, excluding the known foreground galaxies.

camera. Spectroscopically confirmed members are marked by squares, while spectroscopically known foreground galaxies at $z = 0.05$–0.78 from Hasinger et al. (1998b) are marked by circles. The error bars near the bottom of the plot indicate the size of 1σ error. The dotted line marks the 5σ limit in $I-K$ color, while the dashed line shows the CM relation of Coma (Stanford et al. 1998) transformed to the cluster redshift assuming no evolution. The solid line is a linear fit, $(I-K) = (4.201 \pm 0.069) - (0.106 \pm 0.086)(K-18.5)$, to the CM relation of galaxies with $K<20$, $I-K>3$, and $I-K<6$, excluding the known foreground galaxies. There is an indication that the red sequence in RX J1053.7+5735 lies ~0.3 to the blue of the Coma line, qualitatively consistent with previous studies investigating other clusters at $z \sim 1$ using optical-NIR color and, unlike our study, pre-selection of early-type galaxies by their morphologies (e.g. Stanford et al. 1998; vanDokkum et al. 2001; Stanford et al. 2002; Holden et al. 2004). There is also an indication that the fitted slope may be similar to the Coma line, which is consistent with some high redshift studies (e.g. Blakeslee et al. 2003; Lidman et al. 2004), while contradicting studies reporting the slope evolution (e.g. van Dokkum et al. 2001; Stanford et al. 2002). Caution has to be exercised, however, in interpreting our CM diagram, because of the limitation of the data and due to the lack of morphological preselection.

3.2. Spectral properties

Figures 3 and 4 show optical spectra of cluster members in the eastern and western subclusters, respectively. Sky emission and absorption spectra are shown at the bottom and the top of the figure, respectively, with arbitrary flux levels. Subtraction of sky *emission* lines is relatively good, considering the faint magnitude of the objects. The spectra of Objects 1 and 2 show slightly lower sky-subtraction quality, because they are both observed through a highly tilted slit. Meanwhile, some telluric (i.e. sky absorption) features are eminent, due to the lack of multiplicative sky correction, which is not practical for faint galaxy spectra. Positions of major spectral features are marked by vertical lines. Solid vertical lines represent features used for redshift determination, while dashed lines are plotted for reference. Major spectral absorption features, such as Ca II H and K

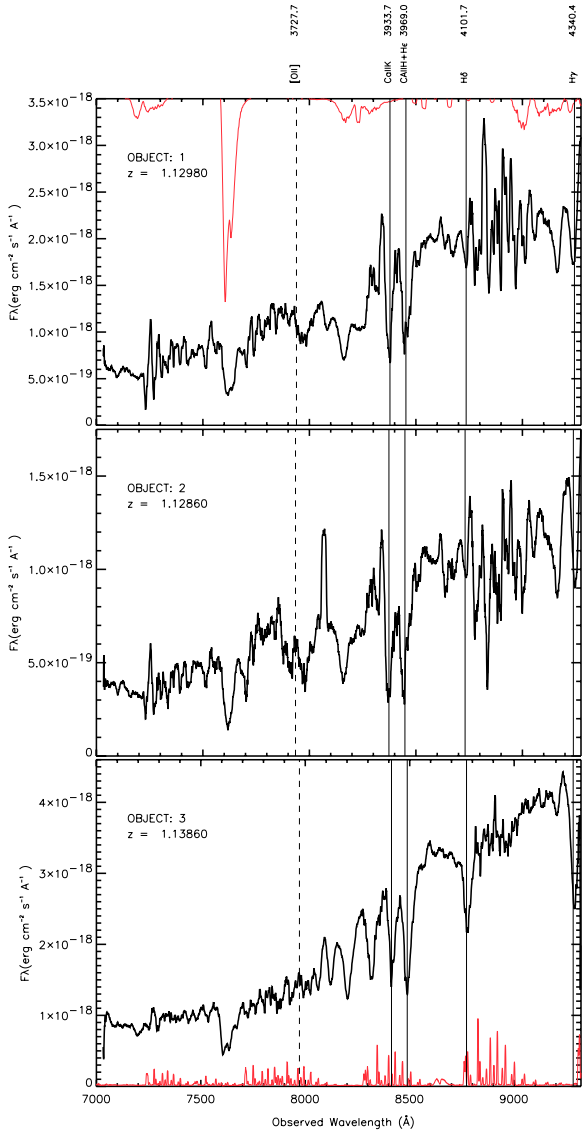

Fig. 3. Optical spectra of eastern members obtained using DEIMOS mounted on Keck telescope. Sky emission and absorption spectra are shown at the bottom and the top of the figure, respectively, with arbitrary flux levels. Positions of major spectra features are marked by vertical lines. Solid vertical lines represent features used for redshift determination, while dashed lines are plotted just as references.

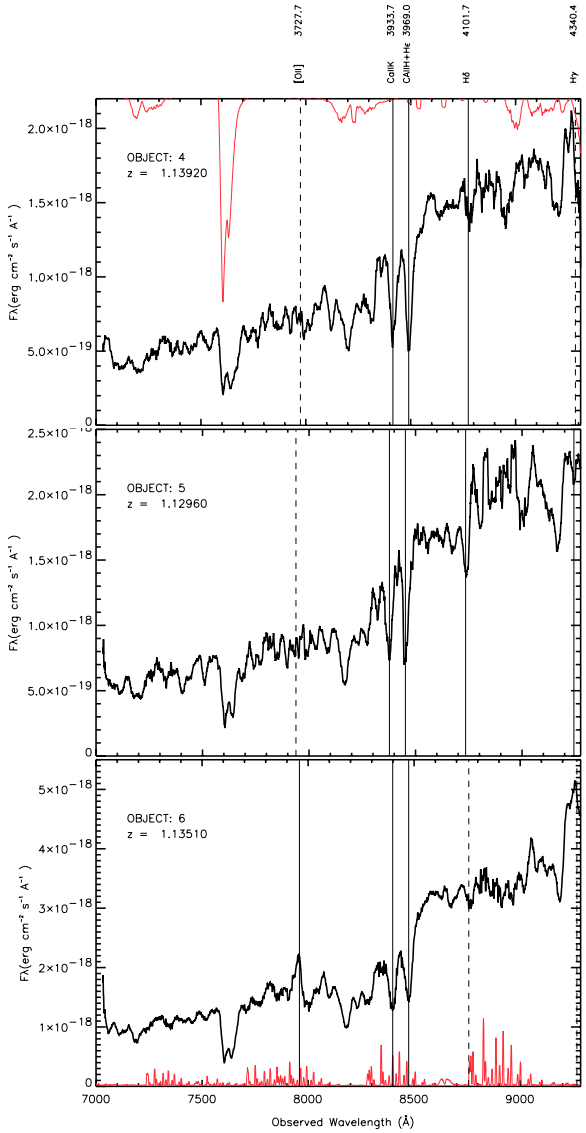

Fig. 4. Optical spectra of western members obtained using DEIMOS. Symbols are the same as Fig. 3.

and several Balmer lines were typically used for this determination. We avoided using a Mg I λ3830 absorption feature because of its proximity to the telluric lines. Redshifts were calculated by centering these major spectral features and then fitting a redshift solution using IRAF *rvidlines* task. Among eight candidate galaxies, six were found to have redshifts in the range $1.129 < z < 1.139$, with a mean redshift $\langle z \rangle = 1.134$ and a line-of-sight velocity dispersion $\Delta v \sim 650$ km s^{-1}. The mean redshift agrees well with the cluster redshift derived from the X-ray spectroscopy by Hashimoto et al. (2004). The velocity dispersion may be consistent with that expected from the cluster X-ray temperature, although caution has to be exercised in interpreting the result because of the uncertainty associated with the dynamical status of the cluster. All six secure members show clear absorption features of CaII H and K and several Balmer lines, typical of early galaxies in the present epoch, and consistent with their $I - K$ colors. An emission-like feature at ~8100 Å of Object 2 is an artifact caused by a cosmic ray that we are unable to completely remove because of its location on a major sky emission line. One additional galaxy in the eastern lobe shows a single emission-like feature in an otherwise featureless spectrum. If we interpret this as a real [OII]λ3727 emission, it may yield a seventh member galaxy at redshift of $z = 1.122$. To be conservative, however, we decided to exclude this galaxy from the cluster membership, because its redshift was estimated by an insecure single feature. For the last (eighth) galaxy we observed, we were unable to obtain a redshift due to the lack of any spectral features.

4. Summary

Using Keck-DEIMOS spectroscopic observations of galaxies in the $2\farcm0 \times 1\farcm5$ region surrounding the X-ray detected cluster candidate RX J1053.7+5735, we secured redshifts for six galaxies in the range $1.129 < z < 1.139$, with a mean redshift $\langle z \rangle = 1.134$. The mean redshift agrees well with the cluster X-ray redshift previously estimated by Hashimoto et al. (2004) using the cluster X-ray Fe-K line, confirming the presence of a cluster at $z \sim 1.135$. Galaxy ID 1 shows a clear redshift $z = 1.13$, consistent with its photometric redshift, but inconsistent with the NIR spectroscopic redshift estimated by Thompson et al. (2001). Galaxies with concordant redshifts are located in both eastern and western sub-clusters of the double cluster structure, indicating that both components are possibly at similar redshifts. This result is also consistent with Hashimoto et al. (2004) where they show that both eastern and western X-ray lobes have similar X-ray redshifts. Based on their separation of ∼250 kpc, these results support the interpretation that RX J1053.7+5735 is an equal-mass cluster merger taking place at $z \sim 1$, although further direct evidence for the dynamical state of the cluster is needed for a more definitive statement about the cluster merging state. The six galaxies have a line-of-sight velocity dispersion $\Delta v \sim 650\,\mathrm{km\,s^{-1}}$, and all six show clear absorption features of CaII H and K and several Balmer lines, typical of early galaxies at the present epoch, in agreement with their $I - K$ colors. A color–magnitude diagram, constructed from deep optical/NIR observations of the RX J1053.7+5735 field, shows a clear red color sequence. There is an indication that the red sequence in RX J1053.7+5735 lies ∼0.3 to the blue of the Coma line, qualitatively consistent with other studies investigating other clusters at $z \sim 1$. There is also an indication that the fitted slope may be similar to the Coma line, consistent with some high redshift studies, while contradicting studies reporting the slope evolution. Caution has to be exercised, however, in interpreting our CM diagram, because of the limitation of the data and due to the lack of morphological pre-selection.

Acknowledgements. We thank the IfA Surf's Up collaborations for their help in acquiring the Subaru data. J.P.H. thanks the Alexander v. Humboldt Foundation for its generous support. We thank Sekyoung Yi and Sugata Kaviraj for helpful information. We acknowledge the referee's comments, which improved the manuscript.

References

Bahcall, N., Fan, X., & Cen, R. 1997, ApJ, 485, L53
Barris, B. J., Tonry, J. L., Blondin, S., et al. 2004, ApJ, 602, 571
Bertin, E., & Arnouts, S. 1996, A&AS, 117, 393
Blakeslee, J. P., Franx, M., Postman, M., et al. 2003, ApJ, 569, 143
Casali, M. M., & Hawarden, T. G. 1992, JCMT-UKIRT Newsletter, 4, 33
Eggen, O. J., Lynden-Bell, D., & Sandage, A. R. 1962, ApJ, 136, 748
Eke, V. R., Cole, S., & Frenk, C. S. 1996, MNRAS, 282, 263
Faber, S. M., Phillips, A. C., Kibrick, R. I., et al. 2003, SPIE, 4841, 1657
Fukugita, M., Ichikawa, T., Gunn, J. E., et al. 1996, AJ, 111, 1748
Hashimoto, Y., Hasinger, G., Arnaud, M., Rosati, P., & Miyaji, T. 2002, A&A, 381, 841
Hashimoto, Y., Barcons, X., Böhringer, H., et al. 2004, A&A, 419, 819
Hasinger, G., Burg, R., Giacconi, R., et al. 1998a, A&A, 329, 482
Hasinger, G., Giacconi, R., Gunn, J. E., et al. 1998b, A&A, 340, L27
Holden, B. P., Stanford, S. A., Esenhardt, P., et al. 2004, AJ, 127, 2484
Kauffmann, G. 1996, MNRAS, 281, 487
Kauffmann, G., & Charlot, S. 1998, MNRAS, 294, 705
Lidman, C., Rosati, P., Demarco, R., et al. 2004, A&A, 416, 829
Lockman, F. J., Jahoda, K., & McCammon, D. 1986, ApJ, 302, 432
Miyazaki, S., Sekiguchi, M., Imi, K., et al. 1998, Proc. SPIE, 3355, 363
Stanford, S. A., Eisenhardt, P. R., & Dickinson, M. 1998, ApJ, 492, 461
Stanford, S. A., Holden, B., Rosati, P., et al. 2002, ApJ, 123, 619
Thompson, D., Pozzetti, L., Hasinger, G., et al. 2001, A&A, 377, 778
van Dokkum, P. G., Stanford, S. A., Holden, B. P., et al. 2001, ApJ, 552, L101